Anal. Methods Environ. Chem. J. 7 (4) (2024) 78-95

AMECJ

Research Article, Issue 4
Analytical Methods in Environmental Chemistry Journal
Journal home page: www.amecj.com/ir

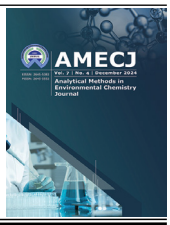

# Zinc adsorption from synthetic wastewater using synthesis activated carbons from sugarcane bagasse and Cashew nut shells before determination by atomic absorption spectrometry

**Yusufu Luka[a, *], Timothy Musa Chiroma[a], Abdulhalim Musa Abubakar[a], and A'aron Donidamini Kachalla[a]**
[a]*Department of Chemical Engineering, Faculty of Engineering, Modibbo Adama University, PMB 2076, Yola, Adamawa State, Nigeria*

**ARTICLE INFO:**

Received 9 Aug 2024
Revised form 13 Oct 2024
Accepted 11 Nov 2024
Available online 30 Dec 2024

**Keywords:**
Zinc,
Activated carbon,
Adsorption,
Atomic absorption spectrometry,
Synthetic Wastewater,
Optimization

**ABSTRACT**

The present study examined its application in removing Zinc (Zn) from synthetic water. The mechanism for the adsorption of Zn by sugarcane bagasse (SCB) and cashew nut shell (CNS) is linked to the role played by the vital stretching functional groups such as hydroxyl (-OH) and other phenol and aromatic groups, as revealed by the Fourier Transform Infrared (FTIR) characterization technique. The existence of porous channels on the activated carbon (AC) revealed by Scanning Electron Microscopy (SEM) and depleted Zn ions in the water after sorption by Atomic Adsorption Spectrometry (AAS) analysis was an added merit. The effect of varying contact time (0-50 min) and initial Zn concentration (30-100 mg $L^{-1}$) resulted in good fits of the predicted adsorption capacity and removal responses (%), described by 3 quadratic and one linear model. Statistical metrics, 3D surface, and contour plots based on Central Composite Design (CCD) Response Surface Methodology (RSM) carried out put CNS-AC ahead of SCB-AC as the most efficient adsorbent for ion removal under shorter and longer contact times. In optimized conditions, the parameters such as initial concentration, contact time, removal, adsorption capacity, and desirability for CNS and SCB were achieved at (98.74 mg $L^{-1}$, 50 min, 98.51%, 7.83 mg $g^{-1,}$ and 0.995) and (77.61 mg $L^{-1}$, 5 min, 95.8529%, 6.01 mg $g^{-1}$ and 0.816), respectively. Where the need to use these adsorbents is found, it is important to consider the abundance of the plant waste in the location or contrive a scheme for their massive production.

## 1. Introduction

In recent years, the contamination of water bodies by heavy metals has emerged as a pressing environmental concern, prompting intensive research into effective and sustainable remediation strategies. Among these heavy metals, zinc (Zn) stands out due to its widespread industrial use and potential detrimental effects on ecosystems and human health [1–3]. Synthetic wastewater, mimicking industrial effluents, often contains elevated concentrations of Zn, necessitating efficient treatment methods for its removal. In this situation, using activated carbons (AC) derived from renewable biomass sources [4, 5] presents a promising avenue for the remediation of Zn-

*Corresponding Author: Yusufu Luka
Email: sufuluka@mau.edu.ng
https://doi.org/10.24200/amecj.v7.i04.345

contaminated water. Several agricultural waste biomass can be harnessed in that direction [6–9]. Synthesis and characterization of AC derived from two abundant agricultural byproducts, sugarcane bagasse (SCB) [10, 11] and cashew nut shell (CNS) [12], for the removal of Zn from synthetic wastewater will address this issue. Targeted characteristics must make their AC a good adsorbent [13]. Apart from that, the abundance of waste materials must be considered. For example, Nigeria produced 1588.97 tons of sugarcane in 2023 [14], which is very low despite its enormous capability [15]. Worldwide production grew from 177.28 to 187.88 million metric tons in 2023 [16, 17]. Kogi state in Nigeria is the largest producer of cashews in the country, but discrepancies exist in reports regarding the volume/number of cashews produced in the country [18–20]. Thus, tonnage and location/availability are essential in selecting sugarcane and cashew waste as biosorbents. If there is a need for large-scale remediation applications using those materials, Brazil and the Ivory Coast, with large outputs, will have a better comparative advantage. The implications of this study extend beyond mere pollution mitigation, encompassing broader environmental sustainability and resource utilization objectives. Apart from water cleansing of heavy metals [21–24], adsorbents have proven effective in addressing air pollution [24–28]. By repurposing agricultural waste materials such as SCB and CNS to produce ACs, this research contributes to the valorization of biomass resources and the reduction of waste accumulation. Additionally, developing efficient and cost-effective adsorbents for Zn removal offers tangible benefits for industries tasked with wastewater treatment [29–31], potentially leading to improved regulatory compliance and reduced environmental impact. Previous studies have demonstrated the efficacy of AC for heavy metal removal; however, comprehensive investigations into the precursor characteristics and optimization of synthesis parameters are still needed to enhance their performance further. Notable studies failed to incorporate the most influential parameters [32–36]. This study partly addresses this research gap by employing Response Surface Methodology (RSM) Central Composite Design (CCD) to optimize the preparation conditions of SCB and CNS-AC, thereby maximizing their efficacy in Zn removal from synthetic wastewater. However, CNS has not been fully recognized as a favorable adsorbent for Zn removal, apart from isotherm and kinetic studies conducted by Kumar et al. (2012) previously [37]. It was done without optimization by elucidating the relationship between precursor characteristics (determined via various laboratory analyses), synthesis parameters (contact time and initial metal concentration), and adsorption performance. Zinc (Zn) is naturally available in water bodies, where an amount exceeding 5 mg $L^{-1}$ would result in Zn poisoning. Implementing a remediation strategy to curb its menace is not difficult using plant-based adsorbents. Due to the promise showcased by sugarcane bagasse (SCB) and cashew nut shell (CNS) activated carbon (AC) in previous studies to eliminate other harmful substances from wastewater [38, 39]. This research aims to provide a valuable understanding of the design and optimization of sustainable CNS and SCB-ACs for Zn metal remediation, thereby contributing to the advancement of environmental science and engineering practices.

## 2. Material and Methods

### *2.1. Production of Activated Carbon*

About 100g of SCB and 200g of CNS were collected from wheelbarrow vendors in Jimeta, Adamawa State of Nigeria, and impurities or foreign materials on them were removed by washing with distilled water. These materials were dried by exposing them to the open environment under the sun, as did Kakom et al. (2023), until a considerable amount of moisture is removed. They were then used to prepare carbon by a process called carbonization. Essentially, SCB and CNS samples were carbonized by heating in an Sx-25-12 muffle furnace at 400 and 600°C, respectively, for one hour to obtain their carbons – similar to the temperature range in Suntharam (2022) and

Guillaume et al. (2019). The carbon obtained was mixed with 10g phosphoric acid and water solution activating agents. A ratio of 1:3 of the carbon to the solution was used before feeding it to WHL-254 oven set at 105 for 24 hours to allow its activation. The AC product produced was washed to remove any remaining impurities and dried at 110°C. After burning, it was hit with distilled water several times before oven-drying at 110-120°C for a few hours to obtain the ACs. Only 4000 mL of distilled water was used for washing and cleaning raw materials. Figure 1 shows a synthesis flow diagram specific to the production of grade AC of CNS and SCB in this study. ACs produced from CNS and SCB were then used as adsorbent to remove Zn from a water sample.

### *2.2. Characterization of AC*

Functional group detection was performed using a PerkinElmer spectrum version 10.4.3 FTIR machine domiciled in Modibbo Adama University Central Laboratory, between 500 and 4000 $cm^{-1}$ transmittances with a PE service. Adsorbent morphology was observed through a SEM and EDX (Gold Testing X-ray) spectrophotometer. In this research, SEM analysis was conducted to produce a high-resolution image of the ACs before and after the Zn adsorption process to ascertain the presence of the heavy metal on the activated surface. EDX and AAS (model: AA500) were carried out for metal concentration after adsorption, . For Zn, the limit of detection (LOD) and the linear range are 1-10 µg $L^{-1}$ and 10-5000 µg $L^{-1}$, respectively.

### *2.3. Zinc Metal-Contaminated Wastewater Treatment*

Raw or contaminated water was initially prepared from the 13 runs data generated from RSM CCD by varying the initial concentration of Zn, Ci, (Factor A: mg $L^{-1}$) and contact time (Factor B: min) and keeping the volume of the solution (V) and adsorbent dosage (M) constant (i.e., V = 0.4 mL and M = 5g). The Design Expert 7.0.0 software generates the runs. Table 1 was generated by the Expert tool after setting the time range to 0-50 min and Ci range to 30-100 mg $L^{-1}$. Essentially, the wastewater or raw water was simulated by injecting a specific concentration of Zn in accordance with every run, forming a solution in the process.

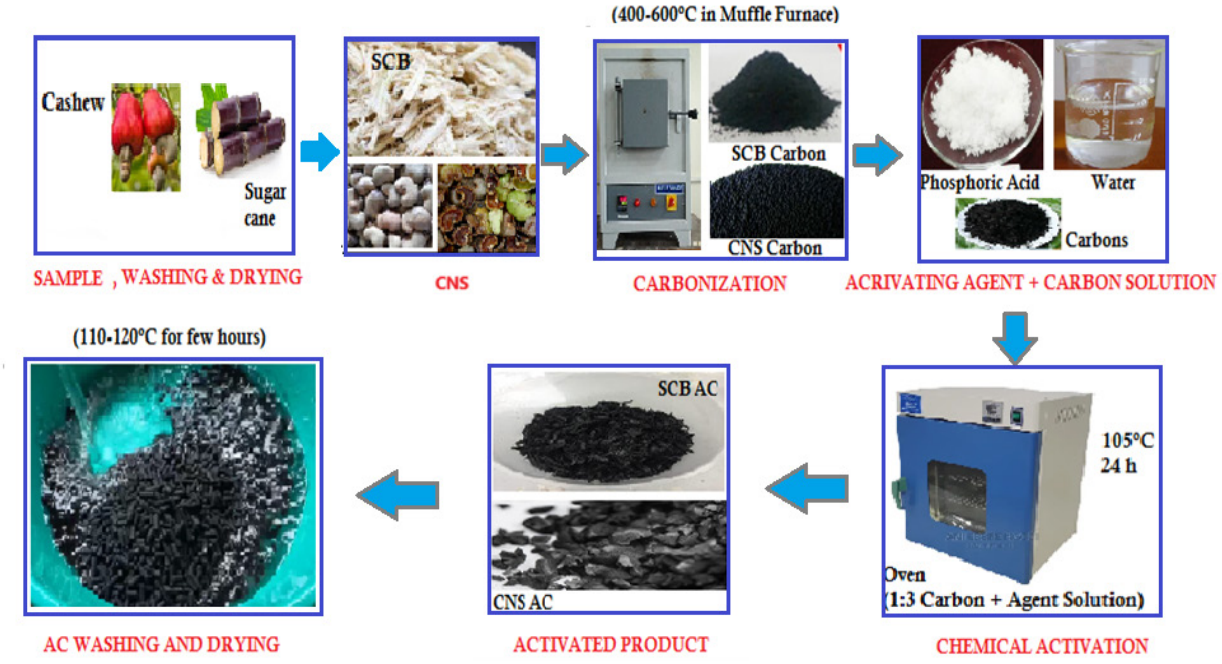


**Fig. 1.** AC Production Steps from SCB and CNS Waste Biomass

**Table 1.** Design of Experiment for Zn Adsorption

| Run | A: Initial Metal Conc. (mg $L^{-1}$) | B: Contact Time (min) |
|---|---|---|
| 1. | 50 | 25.0 |
| 2. | 50 | 46.2 |
| 3. | 50 | 25.0 |
| 4. | 50 | 25.0 |
| 5. | 70 | 40.0 |
| 6. | 78.3 | 25.0 |
| 7. | 70 | 10.0 |
| 8. | 30 | 40.0 |
| 9. | 50 | 25.0 |
| 10. | 50 | 25.0 |
| 11. | 50 | 3.8 |
| 12. | 21.7 | 25.0 |
| 13. | 30 | 10.0 |

### *2.4. EDX and AAS Analysis*

In every run, the AC samples were put in a DFS-KW-1000B water bath shaker according to the run's contact time and filtered using filter paper. This is done to separate the ACs from the water. The experiment was carried out separately using CNS- and SCB-AC. An AAS machine capable of identifying 62 different metals in a solution was used to test for the presence of Zn in the treated water. Other metals were also identified using the EDX machine. Usually, an AAS instrument looks for a particular metal by focusing a beam of UV light at a specific wavelength through a flame and into a detector [40,41]. The sample of interest is aspirated into the flame, and if that metal is present in the sample, it will absorb some of the light, thus reducing its intensity. For the sake of optimization, this final concentration of Zn measured through AAS is used to determine the equilibrium adsorption capacity, qe, (mg $g^{-1}$), and the removal efficiency, RE (% removal), in line with Equations 1 and 2 [42] respectively.

$$q_e = \frac{(C_i - C_e)V}{M} \qquad \text{(Eq.1)}$$

$$RE(\%) = \frac{C_i - C_e}{C_i} \times 100 \qquad \text{(Eq.2)}$$

### *2.5. Optimization*

Calculated RE and qe were then defined as response 1 (R1) and response 2 (R2) to kick-start the CCD statistical analysis, fit and surface plot generation, and optimum selections of contact time and Zn Ci corresponding to a maximum qe and RE. It is carried out for CNS and SCB adsorbent data. Optimization is carried out for two cases. Case 1 is the optimal conditions at a set/specified low contact time where adsorption is expected to be rapid. Case 2 is the optimal conditions at maximum contact time in which adsorption is expected to be slow.

## 3. Results and Discussion

### *3.1. Effect of Specific Functional Groups Present*

The FTIR technique was formerly used to identify the characteristics of the functional groups involved in the adsorption of Zn ions on both the SCB and CNS adsorbent produced. Figure 2 depicts the infrared spectroscopy image of the SCB-AC before and after Zn adsorption from the wastewater. As expected, peaks of various functional groups on the samples are illustrated.

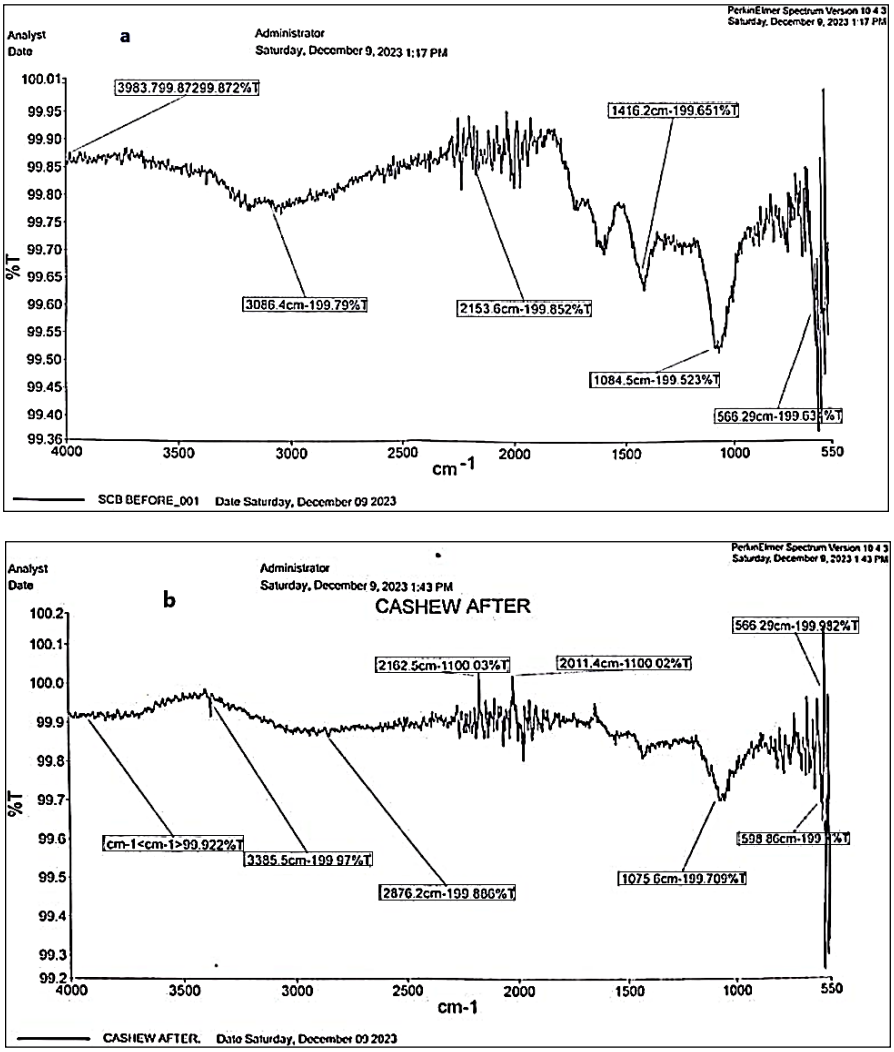


**Fig. 2.** FTIR Spectra of SCB-AC **(a)** Before and **(b)** After Treatment/Adsorption of Zn

In Figure 2a, a peak equivalent to: 3983.799 $cm^{-1}$ could be indicative of O-H stretching vibrations, typically associated with alcohols or phenols [43]; 3086.4 $cm^{-1}$ portrays C-H stretching vibrations often associated with alkanes or alkyl groups; 2153.6 $cm^{-1}$ is quite high for typical functional groups and might be indicative of an instrument-related artifact or an unusual feature; 1416.2 $cm^{-1}$ signifies a C-H bending vibrations usually observed in alkanes; 1084.5 $cm^{-1}$ represents C-O stretching vibrations suggesting the presence of ether or an ester group and; 566.29 $cm^{-1}$ before adsorption, stands for C-Br stretching vibrations, aligning with the presence of an alkyl bromide. Peaks for SCB-AC after adsorption are described as follows: 3809 $cm^{-1}$ suggests the presence of O-H stretching vibrations often associated with alcohol or phenol functional groups; 3347 $cm^{-1}$ indicates N-H stretching vibrations often found in amines or amides; 2532.6 $cm^{-1}$ is a high wave number implying a possible interference or instrument-related artifact; 1596.8 $cm^{-1}$ could be attributed to C=C stretching vibrations in an aromatic ring; 563.33 $cm^{-1}$ is C-Cl stretching vibrations pointing towards the presence of an alkyl chloride and lastly; 886.12 $cm^{-1}$ might be associated with C-H bending vibrations in an aromatic ring or alkane. Secondly, Figure 3 shows the FTIR peaks and wave numbers of the CNS-AC adsorbent showing the functional group before and after Zn adsorption.

Spectrum in Figure 3 presents the characteristic bands corresponding to cellulose besides lignin before Zn adsorption onto CNS-AC, which can be interpreted

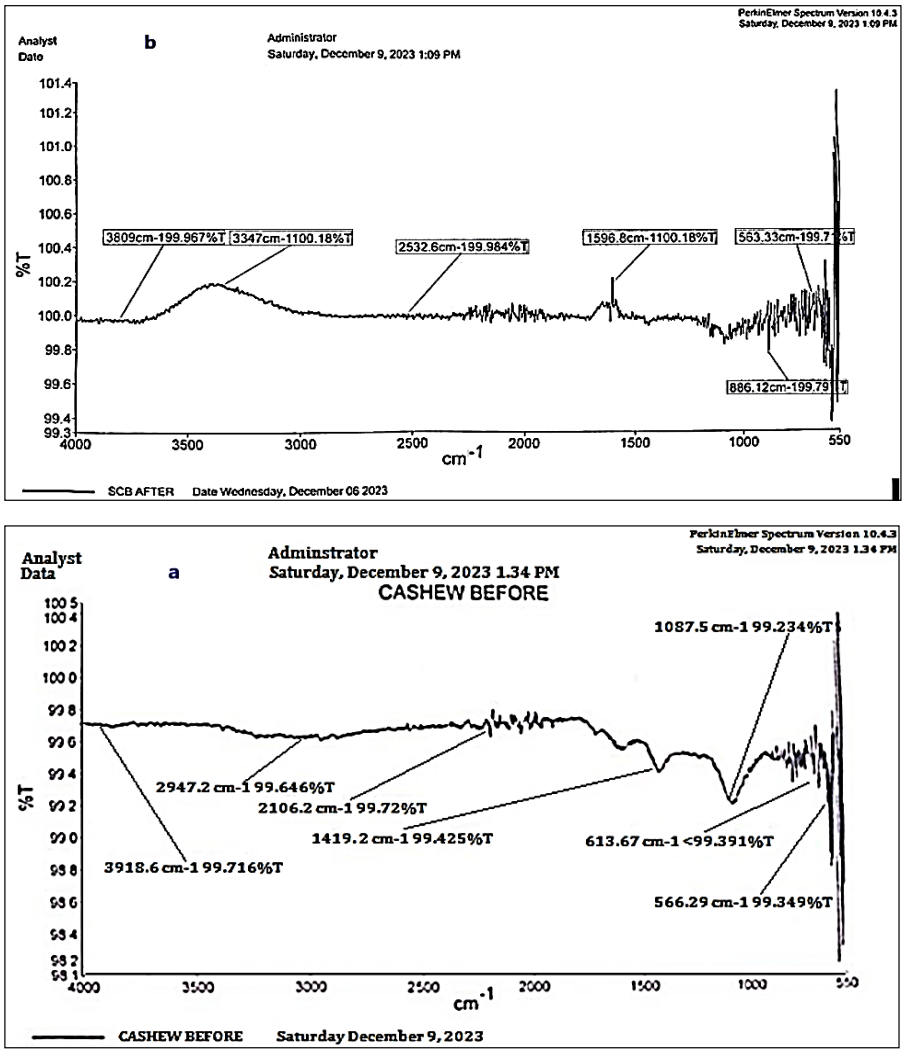


**Fig. 3.** FTIR Spectra of CNS-AC (a) Before and (b) After Treatment/Adsorption of Zn

as follows: 3918.6 $cm^{-1}$ is a broad peak indicative of O-H stretching [44,45], typically associated with alcohol or phenol functional groups; 2947.2 $cm^{-1}$ implied a C-H stretching vibrations often linked to alkanes or alkyl groups; 2106.2 $cm^{-1}$ is a wavelength value that is unusually high for typical functional groups and might be an instrument-related artifact; 1419.2 $cm^{-1}$ correspond to the C-H bending vibrations usually seen in alkanes; 1087.5 $cm^{-1}$ stands for C-O stretching vibrations representing the presence of an ether or an ester group; 613.67 $cm^{-1}$ points to C-Cl stretching vibrations linked to the presence of an alkyl chloride and; 566.29 $cm^{-1}$ illustrates a C-Br stretching vibrations indicating the presence of an alkyl bromide. After adsorption, the peaks shown can be interpreted differently as follows: a peak at 3385.5 $cm^{-1}$ in an FTIR spectrum typically corresponds to the stretching vibration of the O-H (hydroxyl) functional group; 2876.2 $cm^{-1}$ C-H stretching (alkane or alkyl group); 2162.5 $cm^{-1}$ C≡C triple bond stretching (alkyne), also reported in Amoo et al. (2022) 2011.4 $cm^{-1}$ C≡N triple bond stretching (nitrile); 1075.6 $cm^{-1}$ C-O stretching (alcohol or ether); 598.86 $cm^{-1}$ C-Cl stretching (alkyl chloride) and; 566.29 $cm^{-1}$ C-Br stretching (alkyl bromide).

### *3.2. SEM Microstructures and EDX Elemental Compositions*

SEM-EDX analysis of CNS- and SCB-AC before and after Zn ion adsorption are represented in Figures 4 and 5, respectively.

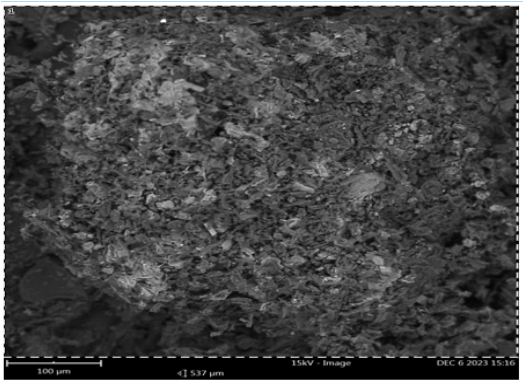

| Element Number | Element Symbol | Element Name | Atomic Conc. | Weight Conc. |
|---|---|---|---|---|
| 6 | C | Carbon | 75.22 | 69.16 |
| 7 | N | Nitrogen | 21.63 | 23.19 |
| 16 | S | Sulfur | 2.17 | 5.33 |
| 19 | K | Potassium | 0.21 | 0.62 |
| 13 | Al | Aluminium | 0.15 | 0.31 |
| 20 | Ca | Calcium | 0.09 | 0.28 |
| 12 | Mg | Magnesium | 0.15 | 0.27 |
| 14 | Si | Silicon | 0.12 | 0.26 |
| 15 | P | Phosphorus | 0.10 | 0.25 |
| 11 | Na | Sodium | 0.11 | 0.20 |
| 17 | Cl | Chlorine | 0.04 | 0.12 |
| 22 | Ti | Titanium | 0.00 | 0.00 |
| 26 | Fe | Iron | 0.00 | 0.00 |

a) FOV: 537 $\mu$m, Mode: 15kV-Image, Detector: BSD Full Time: DEC 6 2023 15:16

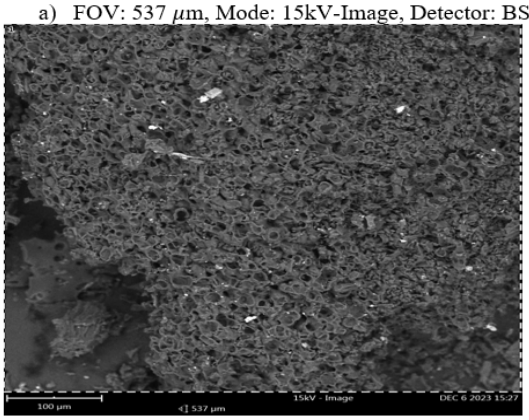

| Element Number | Element Symbol | Element Name | Atomic Conc. | Weight Conc. |
|---|---|---|---|---|
| 6 | C | Carbon | 90.94 | 88.19 |
| 7 | N | Nitrogen | 7.71 | 8.72 |
| 11 | Na | Sodium | 0.34 | 0.63 |
| 16 | S | Sulfur | 0.21 | 0.55 |
| 13 | Al | Aluminium | 0.18 | 0.40 |
| 14 | Si | Silicon | 0.17 | 0.39 |
| 12 | Mg | Magnesium | 0.17 | 0.34 |
| 15 | P | Phosphorus | 0.11 | 0.29 |
| 19 | K | Potassium | 0.06 | 0.19 |
| 20 | Ca | Calcium | 0.05 | 0.16 |
| 17 | Cl | Chlorine | 0.05 | 0.14 |
| 26 | Fe | Iron | 0.00 | 0.00 |
| 22 | Ti | Titanium | 0.00 | 0.00 |

b) FOV: 537 $\mu$m, Mode: 15kV-Image, Detector: BSD Full Time: DEC 6 2023 15:27

**Fig. 4.** SEM-EDX of CNS Adsorbent (**a**) Pre and (**b**) Post-adsorption of Metal

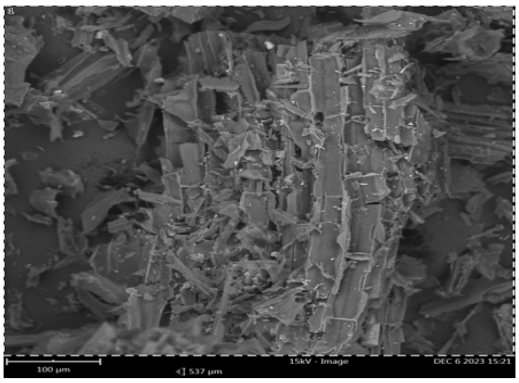

| Element Number | Element Symbol | Element Name | Atomic Conc. | Weight Conc. |
|---|---|---|---|---|
| 6 | C | Carbon | 82.45 | 77.53 |
| 7 | N | Nitrogen | 15.16 | 16.63 |
| 16 | S | Sulfur | 0.84 | 2.11 |
| 14 | Si | Silicon | 0.40 | 0.87 |
| 13 | Al | Aluminium | 0.32 | 0.67 |
| 26 | Fe | Iron | 0.11 | 0.50 |
| 17 | Cl | Chlorine | 0.15 | 0.43 |
| 11 | Na | Sodium | 0.20 | 0.35 |
| 15 | P | Phosphorus | 0.13 | 0.32 |
| 12 | Mg | Magnesium | 0.12 | 0.22 |
| 20 | Ca | Calcium | 0.06 | 0.19 |
| 19 | K | Potassium | 0.06 | 0.17 |
| 22 | Ti | Titanium | 0.00 | 0.00 |

a) FOV: 537 $\mu$m, Mode: 15kV-Image, Detector: BSD Full Time: DEC 6 2023 15:21

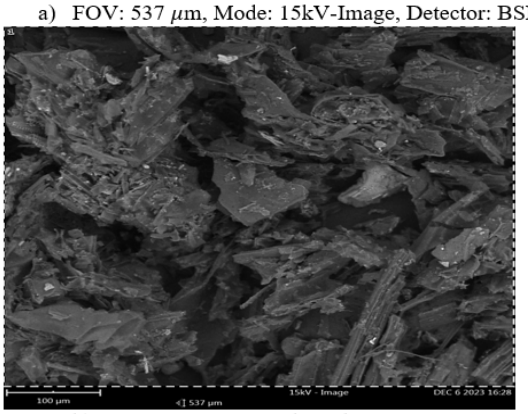

| Element Number | Element Symbol | Element Name | Atomic Conc. | Weight Conc. |
|---|---|---|---|---|
| 6 | C | Carbon | 80.84 | 75.37 |
| 7 | N | Nitrogen | 16.03 | 17.43 |
| 16 | S | Sulfur | 1.02 | 2.54 |
| 14 | Si | Silicon | 0.67 | 1.47 |
| 11 | Na | Sodium | 0.42 | 0.76 |
| 13 | Al | Aluminium | 0.36 | 0.74 |
| 17 | Cl | Chlorine | 0.16 | 0.44 |
| 15 | P | Phosphorus | 0.18 | 0.44 |
| 19 | K | Potassium | 0.13 | 0.38 |
| 12 | Mg | Magnesium | 0.12 | 0.23 |
| 20 | Ca | Calcium | 0.06 | 0.20 |
| 22 | Ti | Titanium | 0.00 | 0.00 |
| 26 | Fe | Iron | 0.00 | 0.00 |

b) FOV: 537 $\mu$m, Mode: 15kV-Image, Detector: BSD Full Time: DEC 6 2023 16:28

**Fig. 5.** SEM-EDX of SCB Adsorbent (**a**) Pre and (**b**) Post-adsorption of Metal

Superficial porous channels were observed in Figures 4a and 5a for CNS and SCB SEM images, respectively, with a spongy adsorbent surface. After adsorption, an irregular morphology was evidenced in Figures 4b and 5b. An alkaline activating agent could be the reason behind the fiber swelling and rupture, thereby favoring the appearance of pores. SEM photograph shows that the AC has a wide variety of pores [46,47] along with the fibrous structure. The shiny surface spotted in the SEM figures is due to the reaction of the impregnating agent (phosphoric acid). It is also observed that the particle sizes are irregular, containing a high surface area available for adsorption of the adsorbate. As a result of carbonization and activation, volatiles are removed, producing a fixed carbon mass with wide pore networks observed in AC samples. The presence of micro-pores contributed to the adsorption occurrence [10]. Alongside the images in Figures 4 and 5 is the metallic elemental composition present in the biomass AC samples before and after biosorption. EDX of CNS-AC reveals a reduction in K (0.62-0.19) and Ca (0.28-0.16 ppm) weight concentrations after adsorption with no evidence of the presence of Zn, as shown in Figure 4. However, only Fe was adsorbed by SCB-AC due to a reduction in its weight concentration from 0.5-0.00 mg L-1(ppm), as showcased in Figure 5, with no Zn detected. This is in consonance with Sawasdee & Watcharabundit's study, which collectively affirmed the possibility of removing Fe from wastewater using SCB and SCB-AC. The presence of Zn ion (after sorption, i.e.,Ce) can be ascertained using the AAS machine since the initial values were already specified for several runs by Desing Expert 7.0.0.

### *3.3. Design-Expert Analysis*

#### *3.3.1.Design Response Table*

Responses in Tables 2 and 3 are computed using the Ce of Zn using Equations 1 and 2 for each run. The mean and standard deviations (SD) of the Ci used are 50 and 15.688 mg $L^{-1}$, and the contact time is 25 and 11.766 mins. The mean and standard division of R1 values for SCB-AC treatment computed is 95.16 and 1.898%, and R2 is 3.82 and 1.232 mg $g^{-1}$, with a ratio of 1.075 and 3.753, respectively. Mean and standard division of R1 values for CNS-AC treatment computed are 94.561 and 3.359%, and R2 is 3.819 and 1.284 mg $g^{-1}$, with a ratio of 1.132 and 4.079, respectively. In Table 2, the optimal values from the design matrix for the responses are 97.229% and 6.002 mg $g^{-1}$ at 25min contact time for 5.0 g of adsorbent dosage.

**Table 2.** Experimental Data for Adsorption Capacity and RE of SCB-AC Adsorbent

| Run | A: ($mgL^{-1}$) | B: time (min) | ($mgL^{-1}$) | R1:RE (%) | R2:qe(mg $g^{-1}$) |
|---|---|---|---|---|---|
| 1. | 50 | 25 | 1.88 | 96.24 | 3.8496 |
| 2. | 50 | 46.21 | 3.12 | 93.76 | 3.7504 |
| 3. | 50 | 25 | 1.88 | 96.24 | 3.8496 |
| 4. | 50 | 25 | 1.88 | 96.24 | 3.8496 |
| 5. | 70 | 40 | 3.45 | 95.07 | 5.3240 |
| 6. | 78.28 | 25 | 3.26 | 95.84 | 6.0016 |
| 7. | 70 | 10 | 1.94 | 97.23 | 5.4448 |
| 8. | 30 | 40 | 2.87 | 90.43 | 2.1704 |
| 9. | 50 | 25 | 1.88 | 96.24 | 3.8496 |
| 10. | 50 | 25 | 1.88 | 96.24 | 3.8496 |
| 11. | 50 | 3.79 | 1.76 | 96.48 | 3.8592 |
| 12. | 21.72 | 25 | 1.73 | 92.03 | 1.5992 |
| 13. | 30 | 10 | 1.66 | 94.47 | 2.2672 |

**Table 3.** Experimental Data for Adsorption Capacity and RE of CNS-AC Adsorbent

| Run | A: (mg $L^{-1}$) | B: Time (min) | (mg $L^{-1}$) | R1:RE (%) | R2: qe(mg $g^{-1}$) |
|---|---|---|---|---|---|
| 1. | 50 | 25.0 | 2.15 | 95.7 | 3.828 |
| 2. | 50 | 46.2 | 1.45 | 97.1 | 3.884 |
| 3. | 50 | 25 | 2.15 | 95.7 | 3.828 |
| 4. | 50 | 25 | 2.15 | 95.7 | 3.828 |
| 5. | 70 | 40 | 1.89 | 97.3 | 5.449 |
| 6. | 78.3 | 25 | 1.15 | 98.5 | 6.171 |
| 7. | 70 | 10 | 2.99 | 95.7 | 5.361 |
| 8. | 30 | 40 | 3.52 | 88.3 | 2.118 |
| 9. | 50 | 25 | 2.15 | 95.7 | 3.828 |
| 10. | 50 | 25 | 2.15 | 95.7 | 3.828 |
| 11. | 50 | 3.8 | 2.15 | 95.7 | 3.828 |
| 12. | 21.7 | 25 | 2.81 | 87.1 | 1.513 |
| 13. | 30 | 10 | 2.67 | 91.1 | 2.186 |

### *3.3.2.ANOVA for Suggested Model*

For R1-SCB-AC data, the model F-value of 48.98 implies that the model is significant. There is only a 0.01% chance that a "model F-value" this large could occur due to noise. Values of "Prob > F" less than 0.05 indicate that model terms are significant [48]. In this case, B, $A^2$ & $B^2$ are significant model terms. Values > 0.1000 indicate that the model terms are not significant [43]. If there are many insignificant model terms (not counting those required to support hierarchy), model reduction may improve the model. For R2-SCB-AC data, the model F-value of 14778.32 implies that the model is significant. There is only a 0.01% chance that a "Model F-value" this large could occur due to noise. Values of "Prob > F" < 0.0500 also indicate significant model terms [34]. Also, A, B, $A^{2,}$ and $B^2$ are significant model terms. The foregone explanation of the R1 & R2 SCB analysis of variance (ANOVA) in Table 4 was given by the Design Expert's 7.0.0 description. Ideally, Factors A and B and Response R1 and R2 were entered for the RSM, and different numerical models, including 2FI, linear, quadratic, and cubic models, were analyzed electronically for best fit. Hence, ANOVA for the suggested best model fit (i.e., quadratic in this study) is shown in Table 4.

Model F-value of 29.59 for R1-CNS-AC data implies that the model is significant, where there is only a 0.01% chance that a "model F-value" this large could occur due to noise. [49,50]. In addition, values of "Prob > F" < 0.0500 signify a significant model term. Hence, $A^2$ is a considerable model term. The Design Expert tool explains that values > 0.1000 correspond with insignificant model terms. If many insignificant model terms exist except those supporting hierarchies, model reduction may improve the R1 model equation generated. The same applies to the R2-CNS-AC data in Table 4, where 'A' is a significant model term. The quadratic models discussed are given by Equations 3-6.

$$RE_{SCB} = \begin{matrix} 87.01978 + 0.34315A - 0.02472B + 0.00156349AB \\ -0.00302385A^2 - 0.00274211B^2 \end{matrix} \quad \text{(Eq.3)}$$

$$q_{eSCB} = \begin{matrix} -0.24067 + 0.085202A + 0.00293825B - 2 \times 10^{-5}AB \\ -6.2135 \times 10^{-5}A^2 - 1.00682 \times 10^{-4}B^2 \end{matrix} \quad \text{(Eq.4)}$$

$$RE_{CNS} = \begin{matrix} 79.31225 + 0.55177A - 0.17201B + 0.00367063AB \\ -0.00456767\ A^2 - 1.10703 \times 10^{-4}B^2 \end{matrix} \quad \text{(Eq.5)}$$

$$q_{eCNS} = -0.29291 + 0.081829A + 8.26658 \times 10^{-4}B \quad \text{(Eq.6)}$$

**Table 4.** ANOVA for Response Surface Quadratic Model of SCB and CNS Data

**SCB**

| Source | Sum of Squares | | df | | Mean Square | | F value | | p-value (Prob > F) | |
|---|---|---|---|---|---|---|---|---|---|---|
| | R1 | R2 | R1 | R2 | R1 | R2 | R1 | R2 | R1 | R2 |
| Model | 45.54 | 19.73 | 5 | 5 | 9.11 | 3.95 | 48.98 | 14778.3 | < 0.0001* | < 0.0001* |
| A- | 0.11 | 5.24 | 1 | 1 | 0.11 | 5.24 | 0.57 | 19602.0 | 0.4763 | < 0.0001 |
| B-Time | 3.07 | 0.00977 | 1 | 1 | 3.07 | 0.00977 | 16.51 | 36.57 | 0.0048 | 0.0005 |
| AB | 0.88 | 0.00014 | 1 | 1 | 0.88 | 0.00014 | 4.73 | 0.54 | 0.0661 | 0.4866 |
| $A^2$ | 10.17 | 0.00430 | 1 | 1 | 10.17 | 0.00430 | 54.71 | 16.08 | 0.0001 | 0.0051 |
| $B^2$ | 2.65 | 0.00357 | 1 | 1 | 2.65 | 0.00357 | 14.23 | 13.36 | 0.007 | 0.0081 |
| Residual | 1.3 | 0.00187 | 7 | 7 | 0.19 | 0.00026 | | | | |
| Lack of Fit | 1.3 | 0.00187 | 3 | 3 | 0.43 | 0.00062 | | | | |
| Pure Error | 0.0 | 0.000 | 4 | 4 | 0 | 0 | | | | |
| Cor Total | 46.84 | 19.74 | 12 | 12 | | | | | | |

**CNS**

| Source | Sum of Squares | | df | | Mean Square | | F value | | p-value (Prob > F) | |
|---|---|---|---|---|---|---|---|---|---|---|
| | R1 | R2 | R1 | R2 | R1 | R2 | R1 | R2 | R1 | R2 |
| Model | 140.05 | 21.43 | 5 | 2 | 28.0 | 10.71 | 29.59 | 5926.22 | 0.0001* | < 0.0001* |
| A- | 2.21 | 21.42 | 1 | 1 | 2.21 | 21.42 | 2.33 | 11851.7 | 0.1707 | < 0.0001 |
| B-Time | 3.16 | 0.00123 | 1 | 1 | 3.16 | 0.00123 | 3.33 | 0.68 | 0.1106 | 0.4287 |
| AB | 4.85 | | 1 | | 4.85 | | 5.12 | | 0.058 | |
| $A^2$ | 23.21 | | 1 | | 23.2 | | 24.52 | | 0.0017 | |
| $B^2$ | 0.00431.0 | | 1 | | 0.00431 | | 0.00456 | | 0.9481 | |
| Residual | 6.63 | 0.018 | 7 | 10 | 0.95 | 0.00181 | | | | |
| Lack of Fit | 6.63 | 0.018 | 3 | 6 | 2.21 | 0.00301 | | | | |
| Pure Error | 0.0 | 0.00 | 4 | 4 | 0.00 | 0.00 | | | | |
| Cor Total | 146.68 | 21.44 | 12 | 12 | | | | | | |

* *implied 'significant'*

Only Model Equation 6 is linear. Ogundeji & Jimoh (2021) obtained a 4-factor quadratic model for $RE_{SCB}$ Comprising of time, pH, temperature, and dosage. Predicted $R^2$ of 0.8024 for $RE_{SCB}$ (Table 5) is in reasonable agreement with its adjusted $R^2$ of 0.9524. A ratio > 4 (19.469) is desirable for adequate precision in measuring the signal-to-noise ratio. Because of this adequate signal, Model Equation 3 can be used to navigate the design space.

The same faith is observed for $RE_{SCB}$ with larger sets of $R^2$ values, demonstrating a better fit by model Equation 4. Not as expected, predicted $R^2$ of 0.6788 for $RE_{SCB}$ is not as close to the adj. $R^2$ = 0.9226, portraying a significant block effect or possible model issues and data. Things to consider are model reduction, response transformation, outliers, etc. Adeq. precision that measures the signal-to-noise ratio is > 4 (i.e., 18.168) and desirable, implying an adequate signal [36]. Model Equation 5 can thus be used to navigate the design space. There is, however, a reasonable agreement between the predicted $R^2$ = 0.9982 and the adj. $R^2$ = 0.9990 for qe CNS. A desirable signal-to-noise ratio (Adeq Prec = 226.605 > 4) was achieved, showing that Model Equation 6 can navigate the design space due to the adequate signal it portrays.

**Table 5.** Statistics results of SCB-AC and CNS-AC models

| Parameter | SCB-AC | | CNS-AC | |
|---|---|---|---|---|
| | R1 | R2 | R1 | R2 |
| Std. Dev. | 0.43 | 0.016 | 0.97 | 0.043 |
| Mean | 95.12 | 3.82 | 94.56 | 3.82 |
| C.V. % | 0.45 | 0.43 | 1.03 | 1.11 |
| PRESS* | 9.26 | 0.013 | 47.12 | 0.04 |
| $R^2$ | 0.9722 | 0.9999 | 0.9548 | 0.9992 |
| Adj. $R^2$ | 0.9524 | 0.9998 | 0.9226 | 0.999 |
| Pred. $R^2$ | 0.8024 | 0.9993 | 0.6788 | 0.9982 |
| Adeq Prec. | 19.469 | 399.846 | 18.168 | 226.605 |

* PRESS: Predicted Residual Sum of Squares

SD mean and coefficient of variation (C.V.%) are measures of the model's precision and accuracy. The PRESS (Predicted Residual Sum of Squares) measures the model's predictive ability. For the R1 and R2 responses of SCB-AC and CNS-AC, the mean values are close to 95% and 3.8 mg $g^{-1}$, respectively, indicating that the models can predict the response values accurately. Also observed are low SD values, indicating that the data points are close to the mean and the model is precise; low CV(%) values, indicating that the precision of the model is high; low PRESS values for the RSM models, indicating that the models have good predictive ability; high $R^2$ values for the models, indicating that the models fit the data well and; high adjusted $R^2$ values [49-52], indicating that the models do not overfit the data. As such, the fit statistics in Table 5 suggest that the RSM models developed for the SCB-AC and CNS-AC data are accurate, precise, and have good predictive ability.

### *3.3.3.3D Optimal Depictions and Extent of Fit*

Figures 6 and 7 provide a comprehensive visual representation of the statistical analysis and optimization of Zn sorption using SCB-AC and CNS-AC adsorbents, respectively. These provide valuable insights for efficient metal removal processes in water treatment applications.

In the 3D surface plot of Figures 6a and 7a, an upward curve indicates an increase in the response variable as the independent variables increase. In this context, the Zn sorption efficiency and capacity (R1 and R2) increase as factors A and B. Respectively, the optimal combination is 39.656 mg $L^{-1}$, 27.12 min, and 96.4375% RE for SCB and 60.175 mg $L^{-1}$, 24.9 min, and 99.35% RE for CNS. Figures 6d and 7d show that as the contact time and Ci both increases, the Zn sorption RE and qe also increases, which means there is a positive relationship between these variables. In addition, the highest Zn RE and qe is achieved at the highest values of both factors, A and B. Thus, the optimal combination occurs at constant time, 71.038 mg $L^{-1}$ and 6.1 mg $g^{-1}$ for SCB, and constant time, 72.245 mg $L^{-1}$ and 6.199 mg $g^{-1}$ for CNS. Figure 6b and 7b contour lines are closely spaced, demonstrating a steep gradient and a strong relationship between the independent variables and the response variable. It also shows that the highest Zn sorption performance is achieved at the highest values of both factors A and B using SCB and CNS-AC. In Figures 6e and 7e, the contour plots show that the highest Zn RE and qe is achieved at intermediate values of both factors A and B. The contour lines are more widely spaced, indicating a weaker relationship between the independent and response variables. Predicted vs. observed RE plot (Figures 6c and 7c) for SCB and CNS outcomes did not fit as perfectly as that in qe relationship (Figure 6f and 7f). Similar REs fit with those in Figures 6c and 7c were obtained by Salihi et al. (2016) using SCB ash to adsorb Zn. Predictions by the four modeled equations are satisfactory, only that those of qe are nearly 100% accurate and precise.

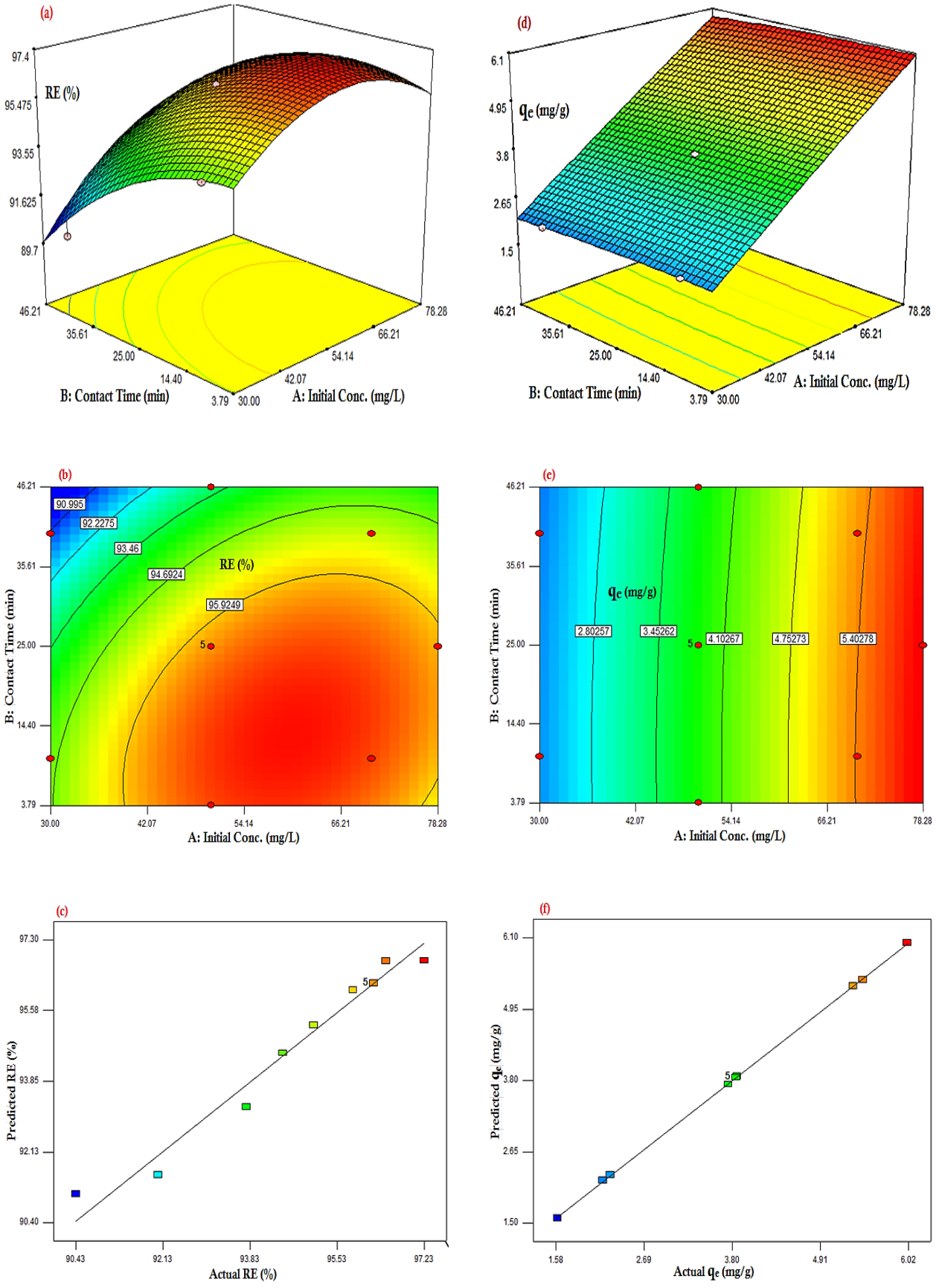


**Fig. 6.** SCB-AC Zn sorption 3D surface, contour, and correlated responses plots

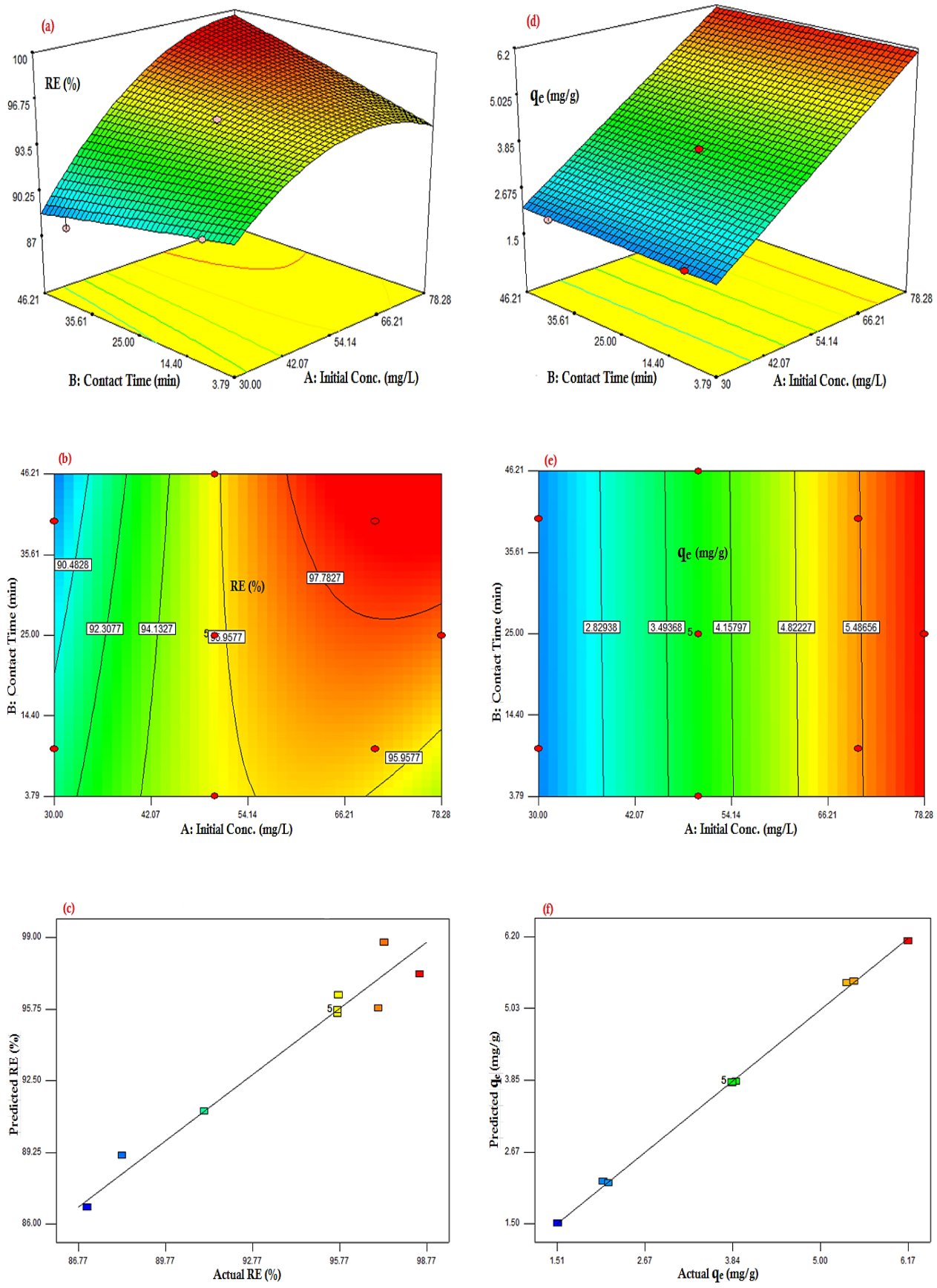


**Fig. 7.** CNS-AC Zn sorption 3D surface, contour, and correlated responses plots

### *3.4. Maximum Adsorption Condition*

Table 6 provides the optimal conditions for Zn sorption for both SCB-AC and CNS-AC adsorbents under different scenarios: rapid and slow adsorption. Rapid means a shorter contact time, while slow means a longer one. Rapid adsorption may be desirable if efficiency is not compromised and cost-effectiveness and practicality are significant concerns. So, at the recovery of SCB-AC (95.85%) and CNS-AC (94.88% ) for Zn sorption, a contact time set at 5 min is desirable given that large amounts of Zn (77.61 and 79.64 mg $L^{-1}$) are sorbed at optimal qe of 6.002 and 6.228 mg $g^{-1}$, respectively. During Zn sorption RSM optimization using SCB where time, dosage, and Ci were varied, Salihi et al. (2016) obtained 55.99%, proving a less efficient process than the one obtained herein. Adamu et al. (2021) surpassed the optimal RE in this study by getting a 100% RE at 5.9895 mg $g^{-1}$ during the SCB-AC Pb removal study. Long contact times (slow adsorption) may be preferable if higher REs are needed, and cost-effectiveness and practicality allow for the extended process duration. This is valid at the given REs for both sorbents in Table 6, with higher qe compared to the rapid sorption situation. Considering both the removal and qe along with the desirability values, CNS is the superior adsorbent for removing Zn in both rapid and slow adsorption conditions, as it consistently demonstrates higher qe desirability values. CNS benefits from longer contact times, showing significantly higher performance and desirability than SCB, especially under slow adsorption conditions. Therefore, an adsorbent dosage of 5.0 g can adsorb approximately 99 mg $L^{-1}$ of Zn from water. It is considered highly effective if an adsorbent maintains high adsorption efficiency across a range of initial Zn concentrations, as does SCB and CNS-AC. When Hasar et al. increased Zn concentration to 200 mg $L^{-1}$, a significant reduction in the RE was witnessed.

## 4. Conclusions

Following laboratory-designed steps, AC was produced from SCB and CNS and used as an adsorbent to eliminate Zn from synthetic water. Changes in peaks recorded after FTIR for both SCB or CNS-ACS and their morphology confirm that the adsorbents have porous regions and active sites for Zn sorption. Characterizing the ACs by running an AAS analysis presents a further reduction in the concentration of Zn below the specified initial values added to the water sample. The CCD optimization RSM type chosen provided experimental runs to quantify qe and RE at different contact times and Zn Ci . These Ci amounts are way above 5.0 mg $L^{-1}$ permissible Zn concentration in water, and the fact that optimization carried out shows that 77.61-98.74 mg $L^{-1}$ optimal value can be removed (at 94.79-98.51% RE) under slow or rapid adsorption hinted to the efficiency of the two analyzed adsorbents for Zn removal. Juxtaposing the adsorbent performance, it was found that CNS-AC is more efficient at removing the ions from synthetic water than SCB-AC. At higher RE, CNS-AC achieved 7.8279 mg $g^{-1}$ adsorption capacity at 99.5% desirability with fitted quadratic model prediction ($R^2$ = 0.9992). Still, qe and RE obtained for SCB-AC are best compared to the RSM findings in the literature. Both ACs are favorable biosorbents for Zn metal. It is recommended that the spent adsorbent be regenerated to maintain a continuous bioremediation process. Optimization shouldn't be restricted to two factors only.

**Table 6.** Optimal Conditions for Zn sorption for both SCB-AC and CNS-AC adsorbents

| Cases: | Optimal Conditions | | | | |
|---|---|---|---|---|---|
| | A (mgL$^{-1}$) | B (min) | R1 (%) | R2 (mg g$^{-1}$) | Desirability |
| | | | **SCB** | | |
| Rapid Adsorption | 77.61 | 5 | 95.8529% | 6.00163 | 0.816 |
| Slow Adsorption | 80.97 | 38.94 | 94.7885 | 6.1494 | 0.776 |
| | | | **CNS** | | |
| Rapid Adsorption | 79.64 | 5 | 94.8826 | 6.2284 | 0.785 |
| Slow Adsorption | 98.74 | 50 | 98.5058 | 7.82794 | 0.995 |

## 5. References


[1] P. S. Kumar, A. Saravanan, K. A. Kumar, R. Yashwanth, S. Visvesh, Removal of toxic zinc from water/wastewater using eucalyptus seeds activated carbon: non-linear regression analysis, IET Nanobiotechnol., 10 (2016) 244–253. https:// doi.org/ 10.1049 / iet-nbt. 2015.0087

[2] R. R. Karri, J. N. Sahu, Modeling and optimization by particle swarm embedded neural network for adsorption of zinc (II) by palm kernel shell based activated carbon from aqueous environment, J. Environ. Manage., 206 (2017) 178–191. https://doi.org/10.1016/j.jenvman.2017.10.026

[3] S. Tuomikoski, Zinc adsorption by activated carbon prepared from lignocellulosic waste biomass, Appl. Sci., 9 (2019) 1–15. https://doi.org/10.3390/app9214583

[4] Y. X. Gan, Activated carbon from biomass sustainable sources, C–J. Carbon Res., 7 (2021) 1–33. https://doi.org/10.3390/c7020039

[5] M. A. Suryawanshi, A. Bandgar, C. Mhaske, S. Shetty, Production of activated carbon from various natural resources and its application, J. Emerg. Technol. Innov. Res., 7 (2020) 560–565.http://www.jetir.org/papers/JETIR2009075.pdf

[6] J. K. Ratan, M. Kaur, B. Adiraju, Synthesis of activated carbon from agricultural waste using a simple method: Characterization, parametric and isotherms study, Mater. Proc., 5 (2018) 3334–3345. https://doi.org/10.1016/j.matpr.2017.11.576

[7] Y. Luka, B. K. Highina, A. Zubairu, The promising precursors for development of activated carbon: Agricultural waste materials-A review, Int. J. Adv. Sci. Res. Eng., 4 (2018) 45–59. https://doi.org/10.7324/IJASRE.2018.32615

[8] A. Bhatnagar, M. Sillanpää, A. Witek-Krowiak, Agricultural waste peels as versatile biomass for water purification–A review, Chem. Eng. J., 270 (2015) 244–271. https://doi.org/10.1016/j.cej.2015.01.135

[9] S. R. Binti Jamaludin, A production of activated carbon using local agricultural waste for groundwater treatment in Universiti Malaysia Pahang, Bachelor of civil engineering degree thesis, Faculty of Civil Engineering and Earth Resources, University Malaysia Pahang, 2010. https://webopac.kmlink.com.my/neuaxis-e/Record/ump-2548

[10] M. A. M. Razi, A. Al-Gheethi, Removal of heavy metals from textile wastewater using sugarcane bagasse activated carbon, Int. J. Eng. Technol., 7 (2018) 112–115. https://doi.org/10.14419/ijet.v7i4.30.22066

[11] S. M. Kakom, N. M. Abdelmonem, I. M. Ismail, A. A. Refaat, Activated carbon from sugarcane bagasse pyrolysis for heavy metals adsorption, Sugar Tech., 25 (2023) 619–629. https://doi.org/10.1007/s12355-022-01214-3

[12] K. B. Cuillaume, N. S. Serpokrylov, A. S. Smolyanichenko, E. G. Cheblakova, V. A. Gorina, Preparation of activated carbon from cashew nut shells for water purification, Russ. J. Non-ferrous Metals, 61 (2020) 112–118. https://doi.org/10.3103/S1067821220010058

[13] G. Kalaba, J. Nyirenda, O. Munyati, Characterisation of activated carbons for removal of organic and heavy metal pollutants from water in resource limited countries, Desalin. Water Treat., 261 (2022) 224–233. https://doi.org/10.5004/dwt.2022.28531

[14] H. Bakker, Sugar cane cultivation and management, Springer Publisher,1999. https://doi.org/10.1007/978-1-4615-4725-9

[15] J.W. Wayagari, G.B. Ayoola, E.D. Imolehin, Economic evaluation of chewing sugarcane production in the central zone of Nigeria. Sugar Tech., 5 (2003)81–84. https://doi.org/10.1007/BF02943771

[16] I. Hamawand, W. P. Da Silva, S. Seneweera, J. Bundschuh, Value proposition of different methods for utilisation of sugarcane wastes, Energies, 14 (2021) 1–30. https://doi.org/10.3390/en14175483

[17] A. C. Wada, A. Abo-Elwafa, M. T. Salaudeen,

L. Y. Bello, E. H. Kwon-Ndung, Sugar cane production problems in Nigeria and some Northern African countries, Direct Res. J. Agric. Food Sci., 5 (2017) 141–160. http://directresearchpublisher.org/aboutjournal/drjafs

[18] G. Odogun, Kogi, largest producer of cashew in Nigeria-Commissioner, Punch, 2023. https://punchng.com/kogi-to-become-cashew-production-hub-government/

[19] The United States Agency for International Development (USAID), subsector assessment of the Nigerian cashew industry, Washington DC, 2002. https://pdf.usaid.gov/pdf_docs/PNACY675.pdf

[20] O. O. Adeigbe, F. O. Olasupo, B. D. Adewale, A. A. Muyiwa, A review on cashew research and production in Nigeria in the last four decades, Sci. Res. Essays, 10 (2015) 196–209. https://doi.org/10.5897/SRE2014.5953

[21] J. Rakhtshah, H. Shirkhanloo, M. D. Mobarake, Simultaneously speciation and determination of manganese (II) and (VII) ions in water, food, and vegetable samples based on immobilization of N-acetylcysteine on multi-walled carbon nanotubes, Food Chem., 389 (2022) 133124. https://doi.org/10.1016/j.foodchem.2022.133124

[22] Z. Karamzadeh, J. Rakhtshah, N. M. Kazemi, A novel biostructure sorbent based on CysSB/MetSB@MWCNTs for separation of nickel and cobalt in biological samples by ultrasound assisted-dispersive ionic liquid-suspension solid phase micro extraction, J. Pharm. Biomed. Anal., 172 (2019) 285–294. https://doi.org/10.1016/j.jpba.2019.05.003

[23] N. Esmaeili, J. Rakhtshah, E. Kolvari, A. Rashidi, Rapid speciation of lead in human blood and urine samples based on MWCNTs@DMP by dispersive ionic liquid-suspension-micro-solid phase extraction, Biol. Trace Elem. Res., 199 (2021) 1–12. https://doi.org/10.1007/s12011-020-02382-7

[24] K. Merchant, M. D. Mobarake, Ultrasound-assisted solid-liquid trap phase extraction based on functionalized multi wall carbon nanotubes for preconcentration and separation of nickel in petrochemical waste water, J. Anal. Chem., 9 (2019) 865–876. https://doi.org/10.1134/s1061934819090090

[25] F. Golbabaei, A. Vahid, A. Faghihi-Zarandi, A novel nano-palladium embedded on the mesoporous silica nanoparticles for mercury vapor removal from air by the gas field separation consolidation process, Appl. Nanosci., 12 (2022) 1667–1682. https://doi.org/10.1007/s13204-022-02366-0

[26] F. Golbabaei, H. Hassani, F. Eftekhar, M. J. Kian, Occupational exposure to mercury: Air exposure assessment and biological monitoring based on dispersive ionic liquid-liquid microextraction, Iran. J. Public Health, 43 (2014) 793–799. https://www.ncbi.nlm.nih.gov/pmc/articles/PMC4475598/

[27] F. Golbabaei, A. Ebrahimi, A. Koohpaei, A. Faghihi-Zarandi, Single-walled carbon nanotubes (SWCNTs), as a novel sorbent for determination of mercury in air, Glob. J. Health Sci., 8 (2015) 273–280. https://doi.org/10.5539/gjhs.v8n7p273

[28] F. Golbabaei, A. Ebrahimi, H. Shirkhanloo, M. R. Baneshi, A. Faghihi-Zarandi, M. J. Kian, Performance comparison survey of multi-walled and single-walled carbon nanotubes for adsorption and desorption of mercury vapors in the air, Iran. Occup. Health J., 10 (2013) 21–31. https://espace.library.uq.edu.au/view/UQ:9d03f02

[29] L. Lupa, L. Cocheci, Heavy metals removal from water and wastewater, heavy metals – recent advances, InTech Open, pp. 1–29, 2023. https://doi.org/10.5772/intechopen.110228

[30] N. A. A. Qasem, R. H. Mohammed, D. U. Lawal, Removal of heavy metal ions from wastewater: A comprehensive and critical review, NPJ Clean Water, 4 (2021) 1–15. https://doi.org/10.1038/s41545-021-00127-0

[31] B. Von Klock, R. S. Patel, Method for removal of heavy metals from water, US006153108A, 2000. https://patents. google.com/ patent/US6153108A/ en

[32] G. Ravindran, M. R. Madhavi, B. S. Abusahmin, Optimization of zinc(II) adsorption using agricultural waste, Int. J. Eng. Technol., 7 (2018) 300–304. https://doi.org/10.14419/ijet.v7i3.34.19212

[33] N. M. Mubarak, Statistical optimization of zinc removal using activated carbon and magnetic biochar, Adv. Environ. Biol., 8 (2014) 686–691. http://www.aensiweb.com/aeb.html

[34] U. K. Garg, H. K. Garg, Optimization of process parameters for metal ion remediation using agricultural waste materials, Int. J. Theor. Appl. Sci., 8 (2016) 17–24. https://www.researchtrend.net/ijtas/pdf/

[35] T. Van Tran, Q. T. P. Bui, T. D. Nguyen, V. T. T. Ho, L. G. Bach, Application of response surface methodology to optimize the fabrication of ZnCl2-activated carbon from sugarcane bagasse for the removal of $Cu_2$, Water Sci. Technol., 75 (2017) 2047–2055. https://doi.org/10.2166/wst.2017.066

[36] S. M. Beyan, S. V. Prabhu, T. T. Sissay, A. A. Getahun, Sugarcane bagasse based activated carbon preparation and its adsorption efficacy on removal of BOD and COD from textile effluents: RSM based modeling, optimization and kinetic aspects, Bioresour. Technol. Reports, 14 (2021) 1–9. https://doi.org/10.1016/j.biteb.2021.100664

[37] P. S. Kumar, S. Ramalingam, R. V Abhinaya, S. D. Kirupha, T. Vidhyadevi, S. Sivanesan, Adsorption equilibrium, thermodynamics, kinetics, mechanism and process design of zinc (II) ions onto cashew nut shell, Can. J. Chem. Eng., 90 (2012) 973–982. https://doi.org/10.1002/cjce.20588

[38] N. M. Suntharam, Removal of zinc (II) ions from industrial wastewater by activated carbon synthesized from mangrove (Rhizophora mangle), Degree of Bachelor of Chemical Engineering, Universiti Sains Malaysia, 2022. https://eprints.usm.my/55589/

[39] G. Farid, J. Carlos Moreno-Piraján, Cashew nut shell biomass: A source for high-performance $CO_2/CH_4$ adsorption in activated carbon J. $CO_2$ Util., 83 (2024) 102799. https://doi.org/10.1016/j.jcou.2024.102799

[40] M. Rezaee. P. Tajer-Mohammad-Ghazvini, Rapid and efficient determination of zinc in water samples by graphite furnace atomic absorption spectrometry after homogeneous liquid-liquid microextraction via flotation assistance, Bull. Chem. Soc. Ethiop., 36 (2022) 1–11. https://doi.org/10.4314/bcse.v36i1.1

[41] M. Khaleghi Abbasabadi, Speciation of cadmium in human blood samples based on $Fe_3O_4$-supported naphthalene-1-thiol-functionalized graphene oxide nanocomposite by ultrasound-assisted dispersive magnetic micro solid phase extraction, J. Pharm. Biomed. Anal.,189 (2020) 113455. https://doi.org/10.1016/j.jpba.2020.113455

[42] B. A. Ezeonuegbu, Agricultural waste of sugarcane bagasse as efficient adsorbent for lead and nickel removal from untreated wastewater: Biosorption, equilibrium isotherms, kinetics and desorption studies, Biotechnol. Reports, 30 (2021) e00614. https://doi.org/10.1016/j.btre.2021.e00614

[43] O. J. Ogundeji, A. Jimoh, Characterization of sugarcane bagasses as a potential treatment of heavy metal effulents by the response surface methodology, Int. J. Pure Appl. Sci., 20 (2021) 1–24. https://www.cambridgenigeriapub.com/wp-content/uploads/2021/06/CJPAS_Vol20_No9_March_2021-1.pdf.

[44] M. B. Genet, A. L. Jembere, G. A. Tafete, Economical adsorbent developed from sugarcane bagasse for zinc (II) removal from wastewater, Water Air Soil Pollut., 233 (2022) 295. https://doi.org/ 10.1007/ s11270-022-05770-y

[45] T. E. Amoo, K. O. Amoo, O. A. Adeeyo, C. O. Ogidi, Kinetics and equilibrium studies of the adsorption of copper(II) ions from industrial wastewater using activated carbons derived from sugarcane bagasse, Int. J. Chem. Eng., 2022 (2022) 6928568. https://doi.org/10.1155/2022/6928568

[46] W. Somyanonthanakun, A. Greszta, A. J.

Roberts, S. Thongmee, Sugarcane bagasse-derived activated carbon as a potential material for lead ions removal from aqueous solution and supercapacitor energy storage application, Sustainability, 15 (2023) 5566. https://doi.org/10.3390/su15065566

[47] S. Sawasdee, P. Watcharabundit, Adsorption of Fe(II) solution by sugarcane bagasse and activated carbon prepared from sugarcane bagasse, Chian. Mai Uni. J. Nat. Sci, Food Appl. Biosci. Innov. Technol., 18 (2019) 190–213. https://doi.org/10.12982/CMUJNS.2019.0015

[48] M. Mutah, K. Akira, A. M. Zaiton, J. Jafariah, S. M. Razman, I. N. Eman, Production of sugarcane bagasse based activated carbon for $Cd_{2+}$ removal using factorial design, Int. J. Innov. Technol. Explor. Eng., 2 (2013) 121–125. https://www.ijitee.org/wp-content/uploads/papers/v2i4/D0541032413.pdf

[49] H. Z. Mousavi, Chromium speciation in human blood samples based on acetyl cysteine by dispersive liquid–liquid biomicroextraction and in-vitro evaluation of acetyl cysteine/cysteine for decreasing of hexavalent chromium concentration, J. Pharm. Biomed. Anal., 118 (2016) 1-8. https://doi.org/10.1016/j.jpba.2015.10.018

[50] I. U. Salihi, S. R. M. Kutty, M. H. Isa, N. Aminu, Process optimization of zinc removal using microwave incinerated sugarcane bagasse ash (MISCBA) through response surface methodology, Res. J. Appl. Sci. Eng. Technol., 12 (2016) 395–401. https://doi.org/10.19026/rjaset.12.2378

[51] A. D. Adamu, U. A. Abubakar, B. S. Sani, A. Umar, Modelling and optimization of lead adsorption onto sugarcane bagasse activated carbon, Niger. Res. J. Eng. Environ. Sci., 6 (2021) 520–529. http://doi.org/10.5281/zenodo.5805110

[52] H. Hasar, Y. Cuci, E. Obek, M. F. Dilekoglu, Removal of zinc(II) by activated carbon prepared from almond husks under different conditions, Adsorpt. Sci. Technol., 21 (2003) 799–808. https://doi.org/10.1260/026361703607440